Acta Cryst E CRYSTALLOGRAPHIC COMMUNICATIONS

ISSN 2056-9890

Synthesis and crystal structure of *N*-benzyl-5,6-epoxy-7-oxabicyclo[2.2.1]heptane-2,3-dicarboximide

Joseph F. DeJesus,[a] Mary Helene Marmande,[b] Bailey N. Baxter,[b] Masakazu Nambo,[a] Cathleen M. Crudden[a,c] and David C. Forbes[b]*

[a]Institute of Transformative Bio-Molecules (WPI-ITbM), Nagoya University, Nagoya 464-8601, Japan, [b]University of South Alabama, Department of Chemistry, 6040 USA Drive South, Mobile, Alabama 36688, USA, and [c]Queen's University, Kingston, Ontario K7L 3N6, Canada. *Correspondence e-mail: dforbes@southalabama.edu

Received 10 August 2026
Accepted 2 September 2026

Edited by D. R. Manke, University of Massachusetts Dartmouth, USA

Keywords: polycyclic; epoxide; synthesis; stereochemistry; norcanthardin; crystal structure.

CCDC reference: 2585299

Supporting information: this article has supporting information at journals.iucr.org/e

The title compound, $C_{15}H_{13}NO_4$, is an analog of a well-known cytotoxic molecule, canthardin. The compound possesses a 3/5/5/5 contiguous stereo-defined ring network, which features cyclic furan, oxirane and cyclic carboxamide moieties. The flexibility of the *N*-benzyl unit allows for supramolecular chiral (but racemic) packing in the extended crystal structure. The intermolecular interactions in the crystal are dominated by H···H and O···H van der Waals interactions, as shown by Hirshfeld analysis.

1. Chemical context

Compounds based on the 7-oxabicyclo[2.2.1]heptane motif have attracted considerable attention in medicinal chemistry because their conformationally constrained structures can effectively mimic biologically relevant architectures (Scott *et al.*, 2026). This framework is closely related to those present in norcantharidin, a system whose methylated cousin cantharidin has been investigated for anticancer, enzyme-inhibitory, and agrochemical applications (Lawley *et al.*, 2026). Norcanthardin derivatives also possess the advantage of simplicity and scalability of synthesis, for example, by a very straightforward Diels-Alder cyclization (Fig. 1, formation of **1**). In our hands, compound **1** can be isolated in 76% yield in gram quantities by this route, with exclusive *exo* selectivity (Hill *et al.*, 2022). In the 7-oxabicyclo[2.2.1]hept-5-ene core, there is a convenient point of unsaturation to allow for further derivatization (Alves *et al.*, 2023). Using **1** as a common synthon, we were interested

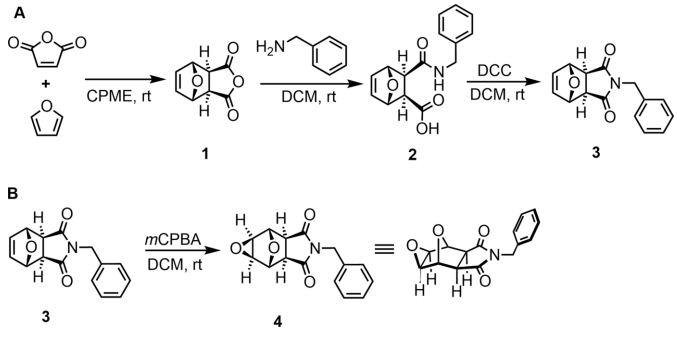

Figure 1
(A) Synthesis of alkene synthon of 7-oxabicyclo[2.2.1]hept-5-ene core (**1**) and transformation of anhydride moiety into more stable 2,3-dicarboximide group (**3**). (B) Transformation of **3** to **4** using *m*CPBA oxidation, and its three-dimensional arrangement with conserved stereochemical control.

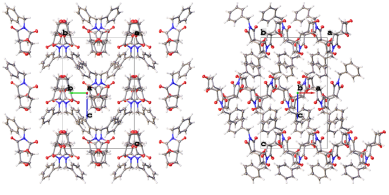

in developing new analogs of norcanthardin to study their biological effects.

This report details the formation and crystallization of the new norcanthardin analog *N*-benzyl-5,6-epoxy-7-oxabicyclo-[2.2.1]heptane-2,3-dicarboximide (**4**). Fig. 1A details the route, which includes nucleophilic ring opening of the anhydride moiety of **1** with benzyl amine to form amidic acid **2**, in 91% yield, and subsequent closing to form the phthalimide **3** with carbodiimide chemistry (79% yield). Compound **3** is a norcanthardin analog with a 5/5/5 tricyclic rigid core and an alkene synthetic handle. Formation of an oxirane moiety through the use of *m*CPBA oxidation chemistry (Fig. 1B) resulted in formation of the highly rigid 3/5/5/5 tetracyclic norcanthardin derivative **4** in 97% yield.

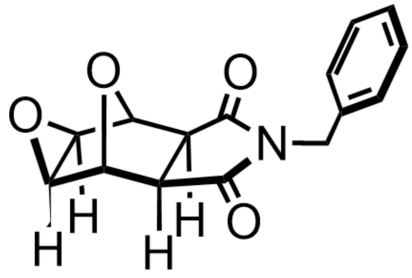

The symmetry of the 3/5/5/5 tetracyclic core and the use of an oxirane functionality in **4** represents both a valuable synthetic intermediate and a versatile platform for further development of biologically active molecules. Furthermore,

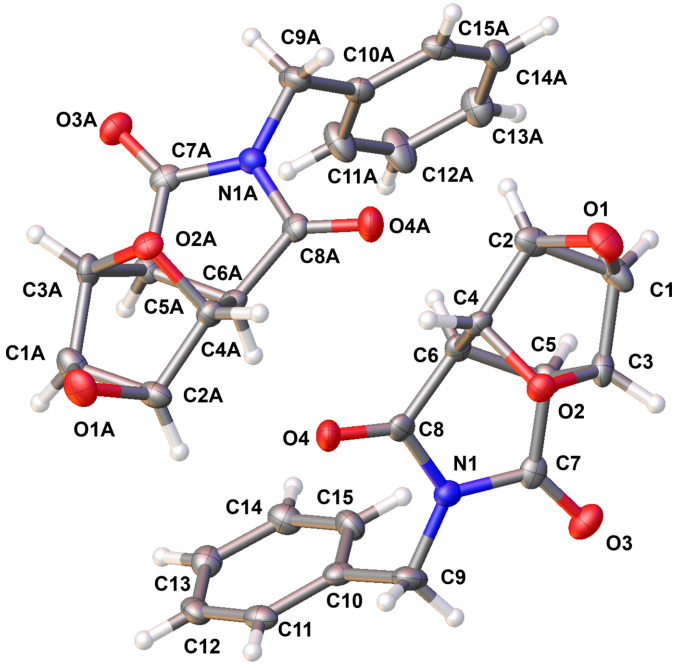

Figure 2
Observed asymmetric unit of **4**, with co-crystallized molecule **4A**. Atom labels for each fragment are shown. Displacement ellipsoids of gray, blue and red correspond to carbon, nitrogen and oxygen, respectively. White spheres correspond to hydrogen atoms.

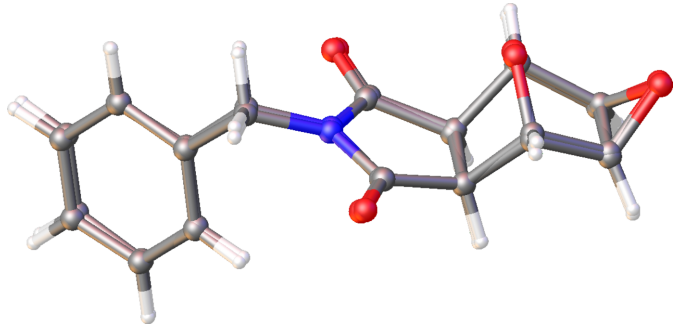

Figure 3
Overlayed molecules in asymmetric unit, **4** and **4A**. Both molecules in the asymmetric unit are nearly identical. Probability ellipsoids shown at 50%.

the rigid scaffold also imposes a well-defined three-dimensional arrangement of functional groups, making this synthon an attractive system for studies of structure–activity relationships and molecular recognition. As such, we sought to characterize the solid-state properties of **4** through X-ray crystallography as an initial attempt to probe structural properties of this new analog.

2. Structural commentary

Compound **4** was crystallized by vapor diffusion of hexanes into a 1.5 mL tube of **4** dissolved in ethyl acetate. Large colorless block-like crystals grew on the sides of the wall of the glass tube. After mounting one of these crystals, the molecular structure of **4** was obtained as shown in Fig. 2. The asymmetric unit of **4** crystallizes in the orthorhombic $Pca2_1$ space group, and has two crystallographically distinct molecules, **4** and **4A**, with no co-crystallized solvent molecules observed. In the course of refining the structure, we found that the absolute configuration of the structure could not be determined reliably. After conducting a Bijovet pairs analysis, we found that the crystal had a 70.1% chance to be an inversion twin. As a result, the crystal was refined as an inversion twin to remedy this issue for further analysis. The rationale for formation of an inversion twin became apparent upon observing the extended crystal structure (*vide infra*, Fig. 4).

Overlaying both molecules in the asymmetric unit (Fig. 3), demonstrates that each fragment is nearly identical, with an alignment RMSD of 0.129 Å. Of note, both fragments have the same contiguous absolute confirguration in the chiral centers (C1/C1*A* = *S*, C2/C2*A* = *R*, C3/C3*A* = *S*, C4/C4*A* = *R*, C5/C5*A* = *S*, C6/C6*A* = *R*), demonstrating that there was no erosion of the starting chirality in the formation of the oxirane unit, or during any of the prior chemical transformations. This results in all four rings of the tetracyclic core 'puckering up', and allowing the oxygen heteroatoms to orient themselves in one direction, which is critical in the cytotoxicity of this family of compounds (Chattopadhyay *et al.*, 2016). Additionally, the ^{1}H NMR spectrum implies that there is only one single stereoisomer present in the bulk of the isolated compound (see Section 5, preparation of **4**).

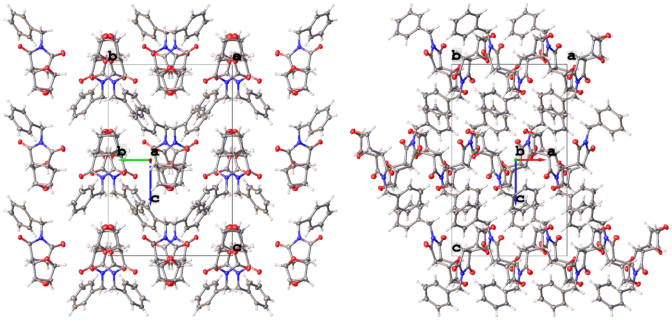

Figure 4
Supramolecular packing of **4**, in a completed unit cell. Left: view of the supramolecular packing looking down the *a* axis. Right: view of the supramolecular packing looking down the *b* axis. Displacement ellipsoids are shown at 50% probability.

3. Supramolecular features

Fig. 4 shows the supramolecular packing of **4** and **4A** down the *a* and *b* axes. Implied by the *Pca2₁* space group, the supramolecular structure shows the two glide-plane operations, where the molecules propagate in a twisting fashion across the crystal. On the edges of the diagram in Fig. 4 left, the *N*-benzyl units are oriented in opposite directions. This alternating orientation of the *N*-benzyl units is shown in both views in Fig. 4 as an apparent packing in the crystal. These alternating *N*-benzyl units explain the two crystallographically distinct molecules in the asymmetric unit, despite the individual molecules being chemically identical when overlain (Fig. 3), since they possess different orientations in the expanded crystal. Because this propagation has a chiral operation, the crystal of **4** crystallizes as a racemic twin due to the presence of the opposite orientation co-crystallizing with this molecule.

Further analyzing the surface contacts in the expanded crystal provides no evidence of classical hydrogen bonding that would explain the intermolecular interactions. We conducted both a two- and a three-dimensional Hirshfeld analysis to probe the types of other intermolecular interactions (such as Van der Waals) within the crystal of **4**, with details summarized in Table 1, Fig. 5 and Fig. 6. The majority of the surface atom contacts were assigned to H···O atoms (43.3%), H·H atoms (39.6%) and H···C atoms (14.8%) as shown in Table 1 and two-dimensional Hirshfeld plots in Fig. 4. This is further shown by the three-dimensional Hirshfeld view, where the strongest indication of surface interactions (in red) is positioned around the epoxide and furan oxygen atoms, and the axial H atoms in the tetracyclic core.

Table 1
Listed surface atom contacts and their percentage contribution to total contacts.

Atom contact	Contribution (%)
H···O/O···H	43.3
H···H	39.6
H···C/C···H	14.8
H···N/N···H	1.1
O···O	0.7
C···O/O···C	0.6

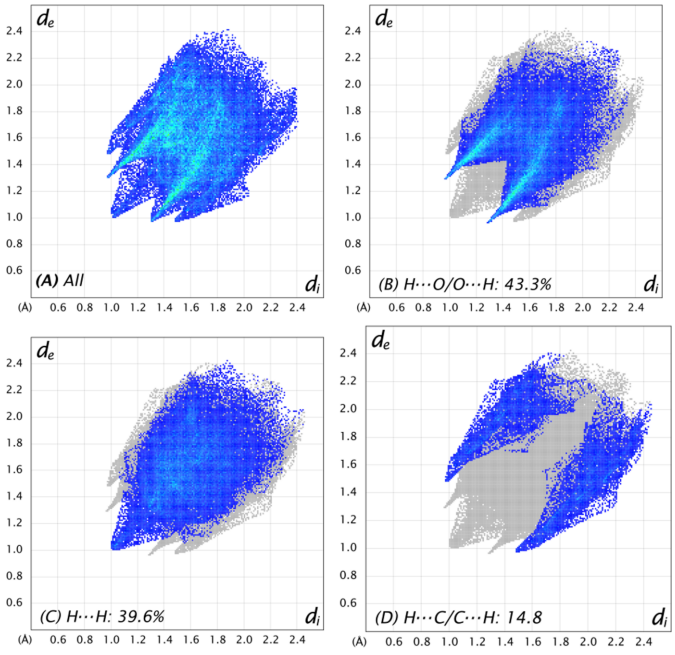

Figure 5
Two-dimensional Hirshfeld Plots of all surface contacts (A) and of the greatest atomic contact contributors of (B) H···O/O···H contacts, (C) H···H contacts and (D) H···C contacts. The brighter blue color shows greater abundance of surface interactions.

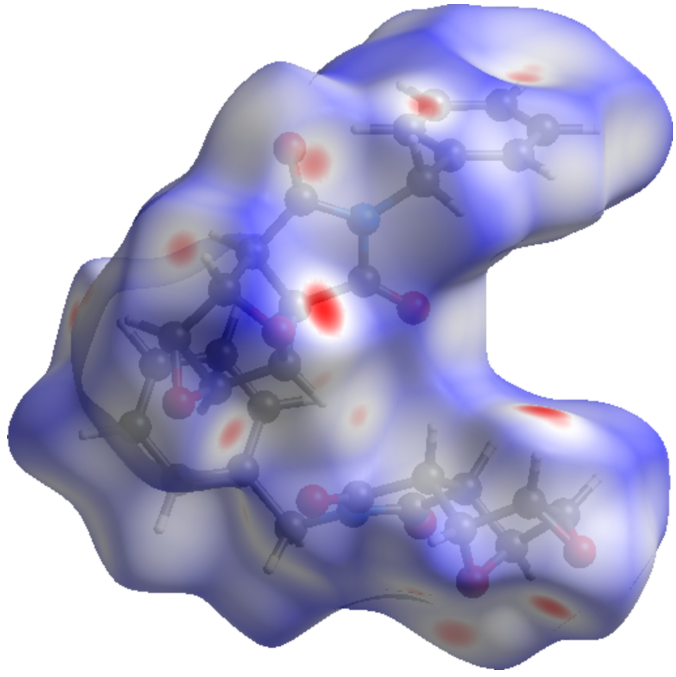

Figure 6
Three-dimensional Hirshfeld surface of the asymmetric unit of **4**, plotted over d_{norm} in the range −0.2533 to 1.3970 a.u. The darker red spheres show the greatest amount of intermolecular surface interactions for specific atoms.

4. Database survey

A database survey (CSD, July 2026; Groom *et al.*, 2016) with the tetracyclic core and the corresponding stereochemistry observed in **4** revealed only one other structure (Ren *et al.* 2026, CCDC: 2486893), with an *N*-3,5-dichlorophenyl substituent rather than an *N*-benzyl substituent in **4**.

5. Synthesis and crystallization

All reactions were conducted under air in ambient conditions unless otherwise stated. All solvents were reagent grade and used as received. ^{1}H and ^{13}C{^{1}H} NMR were conducted on a JEOL ECA-II 400 MHz and JEOL ECA-II 600 MHz spectrometers. All ^{1}H and ^{13}C{^{1}H} NMR spectra were referenced to the residual solvent signal of $CDCl_3$ at 7.26 and 77.16 ppm, respectively. IR spectra were obtained from a JASCO FT/IR-6600 spectrometer using the neat solid compounds. Melting point temperatures were collected on an OptiMelt MPA100 melting point apparatus.

*7-Oxabicyclo[2.2.1]hept-5-ene-2,3-dicarboxylic anhydride (**1**)*

To a 100 mL round-bottomed flask (RBF) equipped with a septum and stir bar and containing maleic anhydride (8.0 g, 81.6 mmol, 3 equiv.) was added 40 mL cyclopentyl methyl ether (CPME). The mixture was externally warmed (318 K) until a solution was formed. After the solution was allowed to cool to room temperature, furan (2.0 mL, 27.5 mmol, 1 equiv.) was added by syringe. The sealed reaction mixture was allowed to stir at room temperature for 3 d at which time, the solid was collected by vacuum filtration and rinsed with diethyl ether (40 mL). Obtained after filtration was a white crystalline solid in 3.5 g (76% yield) and used without further purification. ^{1}H NMR (400 MHz, $CDCl_3$); 6.58 (*s*, 2H, ═CH), 5.47 (*s*, 2H, –CHO–), 3.18 (*s*, 2H, CH).

*3-(Benzylcarbamoyl)-5,6-dihydro-7-oxabicyclo[2.2.1] heptane-2-carboxylic acid (**2**)*

7-Oxabicyclo[2.2.1]hept-5-ene-2,3-dicarboxylic anhydride (**1**) (1.5 g, 8.9 mmol, 1.0 equiv.) was added to a 100 mL RBF equipped with a magnetic stir bar and septum. Dichloromethane (40 mL) was next added to the RBF at room temperature and placed under a blanket of argon. Benzylamine (1.0 mL, 9.4 mmol, 1.05 equiv.) was dissolved in dichloromethane (5 mL) and as a solution, added to the RBF using a disposable Pasteur pipet. The resulting mixture which began forming a precipitant within 5 min of adding the amine was allowed to stir overnight while maintaining the blanket of argon. After adding diethyl ether (20 mL) to the reaction mixture and allowing the slurry to stir for approximately 10 min at room temperature, the solid was isolated by filtration and rinsing with diethyl ether (50 mL). Obtained after filtration was a white crystalline solid in 2.2 g (91% yield) and used without further purification. ^{1}H NMR (400 MHz, $CDCl_3$); 7.32–7.31 (*m*, 5H), 6.79 (*br s*, 1H), 6.48 (*d*, J = 5.2 Hz, 1H), 6.40 (*d*, J = 4.8 Hz, 1H), 5.33 (*s*, 1H), 5.08 (*s*, 1H), 4.43 (*dd*, J = 14.0, 6.0 Hz, 1H), 4.31 (*dd*, J = 14.0, 5.2 Hz, 1H), 2.90 (*d*, J = 9.2 Hz, 1H), 2.82 (*d*, J = 8.4 Hz, 1H).

*N-Benzyl-5,6-dihydro-7-oxabicyclo[2.2.1]heptane-2,3-dicarboximide (**3**)*

After the addition of 3-(benzylcarbamoyl)-5,6-dihydro-7-oxabicyclo[2.2.1]heptane-2-carboxylic acid (**2**) (139 mg, 0.51 mmol, 1.0 equiv.), dichloromethane (DCM) (4.5 mL), dimethylformamide (DMF) (0.50 mL), and 1-hydroxybenzotriazole (HOBt) (86 mg, 0.56 mmol, 1.1 equiv.) to a 10 mL RBF, the solution was externally cooled using an ice bath and placed under a blanket of Ar. A solution of dicyclohexylcarbodiimide (DCC) (116 mg, 0.56 mmol, 1.1 equiv.) in 5 mL of DCM was added dropwise directly into the RBF by syringe. The reaction mixture was allowed to gradually warm to room temperature under a blanket of argon and stir overnight at which time the reaction mixture was filtered through a Celite pad as part of a disposable Pasteur pipet. After the pipet was rinsed with DCM (5 mL), the solution was concentrated *in vacuo* and purified by column chromatography (SiO_2 (10 mm x 80 mm); gradient system EtOAc: hexanes 1:4 (50 mL), 1:2 (50 mL), 1:1 (50 mL); 10 mL fractions collecting tubes 5-14). The isolated material after removal of the volatiles in vacuo was 103 mg [0.40 mmol (79% yield using 3-(benzylcarbamoyl)-5,6-dihydro-7-oxabicyclo[2.2.1]heptane-2-carboxylic acid (**2**) as limiting reactant)]; white solid; ^{1}H NMR (400 MHz, $CDCl_3$); 7.32–7.31 (*m*, 5H), 6.52 (*s*, 2H), 5.30 (*s*, 2H), 4.65 (*s*, 2H), 2.87 (*s*, 2H).

*N-Benzyl-5,6-epoxy-7-oxabicyclo[2.2.1]heptane-2,3-dicarboximide (**4**)*

After the addition of *N*-benzyl-5,6-dihydro-7-oxabicyclo-[2.2.1]heptane-2,3-dicarboximide (**3**) (266 mg, 1.04 mmol, 1.0 equiv.) and dichloromethane (DCM) (2 mL) to a 30 mL (RBF), the solution was externally cooled using an ice bath and placed under a blanket of Ar. A suspension of *m*-chloroperbenzoic acid (*m*CPBA) (359 mg, 2.08 mmol, 2.0 equiv.) in 3 mL of DCM was added after approximately five minutes dropwise directly into the RBF using a disposable Pasteur pipet. [Note: The actual amount weighed was 553 mg factoring the 65% purity.] The vial which contained the *m*CPBA was rinsed and transferred to the RBF using approximately 0.5 mL of DCM. The reaction mixture was allowed to gradually warm to room temperature under a blanket of Ar and stir overnight at which time the excess oxidant was quenched upon addition of a saturated aqueous solution of sodium sulfite (5 mL). After stirring at room temperature for 10 min, the organic phase was washed multiple times to remove 3-chlorobenzoic acid as the reaction was found to go to completion when working with 2.0 equiv. *m*CPBA using a saturated aqueous solution of sodium bicarbonate (3 × 5 mL). The organic layer was next washed with brine, dried over anhydrous magnesium sulfate, and concentrated in vacuo. To obtain analytically pure material, the material was chromatographed (SiO_2 (40 mm × 90 mm); gradient system EtOAc:hexanes 1:1 (100 mL), 2:1 (100 mL), 4:1 (200 mL); 20 mL fractions collecting tubes 9–18). The isolated material after removal of the volatiles in vacuo was 275 mg [1.0 mmol (97% yield using *N*-benzyl-5,6-dihydro-7-oxabicyclo[2.2.1]heptane-2,3-dicarboximide (**3**) as limiting reactant)]; white solid; m.p. 462–463 K. IR (neat, ATR) cm^{-1}:

Table 2
Experimental details.

Crystal data	
Chemical formula	$C_{15}H_{13}NO_4$
M_r	271.26
Crystal system, space group	Orthorhombic, $Pca2_1$
Temperature (K)	143
a, b, c (Å)	11.078 (5), 11.988 (5), 18.432 (8)
V (Å^3)	2447.9 (19)
Z	8
Radiation type	Mo $K\alpha$
μ (mm^{-1})	0.11
Crystal size (mm)	0.31 × 0.20 × 0.14
Data collection	
Diffractometer	Rigaku Pilatus 200K
Absorption correction	Numerical (Busing et al., 1957; Coppens *et al.*, 1965)
T_{min}, T_{max}	0.985, 0.991
No. of measured, independent and observed [$I > 2\sigma(I)$] reflections	37607, 5347, 4234
R_{int}	0.044
(sin $\theta/\lambda)_{max}$ (Å^{-1})	0.649
Refinement	
$R[F^2 > 2\sigma(F^2)]$, $wR(F^2)$, S	0.034, 0.077, 0.92
No. of reflections	5347
No. of parameters	362
No. of restraints	1
H-atom treatment	H-atom parameters constrained
$\Delta\rho_{max}$, $\Delta\rho_{min}$ (e Å^{-3})	0.25, −0.18
Absolute structure	Refined as an inversion twin

Computer programs: *CrystalClear-SM Expert* (Rigaku, 2016), *SHELXT* (Sheldrick, 2015*a*), *SHELXL2019/2* (Sheldrick 2015*b*), *ShelXle* (Hübschle *et al.*, 2011), *OLEX2* (Dolomanov *et al.*, 2009) and CrystalExplorer (Spackman *et al.*, 2021).

2968 (*w*), 1773 (*w*), 1955 (*s*), 1395 (*m*), 1175 (*s*), 1016 (*s*), 859 (*s*), 741 (*s*), 695 (*s*), 585 (*s*).

^{1}H NMR ($CDCl_3$, 600 MHz): δ 7.30–7.26 (*m*, 5H), 4.84 (*s*, 2H), 4.64 (s, 2H), 3.50 (*s*, 2H), 2.99 (*s*, 2H). $^{13}C\{^1H\}$ NMR ($CDCl_3$, 150 MHz): d 175.1, 135.1, 128.7, 128.1, 127.9, 76.7, 49.7, 47.9, 42.8. TLC: Silica gel 60 F_{254} (2:1 ethyl acetate/hexanes); R_f = 0.3.

Crystallization and mounting of ***4***

After dissolving 59 mg of **4** in 1.1 mL of ethyl acetate, 0.4 mL of the solution were placed into a 1.5 mL tube. The tube was then carefully placed into a 20 mL screw-capped vial charged with approximately 6 mL hexanes. After sealing the setup, large colorless block-like and plate crystals formed after 24 h. Crystals were taken directly from mother liquor using a spatula with paratone oil, and dispersed into more paratone oil. The crystal was put on a mounting loop, put on the goniometer head and frozen under a stream of LN_2 (143 K) while data collection was conducted.

6. Refinement

Crystal data collection and structure refinement details are shown and summarized in Table 2. The crystal data was refined as a two-component inversion twin (twin law: [−1, 0, 0, 0, −1, 0, 0, 0, −1]). Due to poor agreement of observed values to calculated values, 5 reflections (1 1 $\overline{3}$, 0 2 $\overline{2}$, 1 2 2, 2 5 $\overline{4}$, 4 4 1) were omitted in the refinement. H atoms were attached to their parent atoms geometrically and constrained to ride on their parent atoms.

Acknowledgements

BNB, MHM, and DCF would like to thank the Department of Chemistry, Honors College, Office of Undergraduate Research, and University of South Alabama Foundation for their generous financial support of undergraduate research. JFD would like to thank Megan Ariki and Aaron Erlich for helping conduct the CSD database survey. JFD would like to thank Matthias Zeller for helpful feedback regarding crystal analysis.

Funding information

Funding for this research was provided by: The Department of Department of Chemistry: Honors College, University of South Alabama's Office of Undergraduate Research; JSPS and Nagoya University through The World Premier International Research Initiative (WPI) program.

References

Alves, T. V. & Fernández, I. (2023). *Org. Biomol. Chem.* **21**, 7767–7775.
Busing, W. R. & Levy, H. A. (1957). *Acta Cryst.* **10**, 180–182.
Chattopadhyay, D., Swingle, M. R., Salter, E. A., Wood, E., D'Arcy, B., Zivanov, C. N., Abney, K., Musiyenko, A., Rusin, S. F., Kettenbach, A., Yet, L., Schroeder, C. E., Golden, J. E., Dunham, W. H., Gingras, A. C., Banerjee, S., Forbes, D. C., Wierzbicki, A. & Honkanen, R. E. (2016). *Biochem. Pharmacol.* **109**, 14–26.
Coppens, P., Leiserowitz, L. & Rabinovich, D. (1965). *Acta Cryst.* **18**, 1035–1038.
Dolomanov, O. V., Bourhis, L. J., Gildea, R. J., Howard, J. A. K. & Puschmann, H. (2009). *J. Appl. Cryst.* **42**, 339–341.
Groom, C. R., Bruno, I. J., Lightfoot, M. P. & Ward, S. C. (2016). *Acta Cryst.* B**72**, 171–179.
Hill, H. P., Baker, N. C., Nguyen, I. B. & Forbes, D. C. (2022). *Journal of Undergraduate Chemistry Research* **21**, 19–24.
Hübschle, C. B., Sheldrick, G. M. & Dittrich, B. (2011). *J. Appl. Cryst.* **44**, 1281–1284.
Lawley, H. K., Baxter, B. N., Lopansri, C. N., Marmande, M. H., Mayeaux, K. N., Orr, L. A. & Forbes, D. C. (2026). *Molbank* M2124.
Ren, Z., Yang, P., Chen, H., Feng, Y., Wu, E., Wang, Z., Chen, Y., Gao, Q. & Wang, J. (2026). *Pestic. Biochem. Physiol.* **219**, 107040.
Rigaku (2016). *CrystalClear-SM Expert*. Rigaku Corporation, Tokyo, Japan.
Scott, K. A., McCluskey, A., Njardarson, J. T. & Wang, W. (2026). *Med. Chem.* **17**, 743–767.
Sheldrick, G. M. (2015*a*). *Acta Cryst.* A**71**, 3–8.
Sheldrick, G. M. (2015*b*). *Acta Cryst.* C**71**, 3–8.
Spackman, P. R., Turner, M. J., McKinnon, J. J., Wolff, S. K., Grimwood, D. J., Jayatilaka, D. & Spackman, M. A. (2021). *J. Appl. Cryst.* **54**, 1006–1011.

supporting information

Acta Cryst. (2026). E**82** [https://doi.org/10.1107/S2056989026009205]

Synthesis and crystal structure of *N*-benzyl-5,6-epoxy-7-oxabicyclo-[2.2.1]heptane-2,3-dicarboximide

Joseph F. DeJesus, Mary Helene Marmande, Bailey N. Baxter, Masakazu Nambo, Cathleen M. Crudden and David C. Forbes

Computing details

N-Benzyl-5,6-epoxy-7-oxabicyclo[2.2.1]heptane-2,3-dicarboximide

Crystal data

$C_{15}H_{13}NO_4$
M_r = 271.26
Orthorhombic, $Pca2_1$
a = 11.078 (5) Å
b = 11.988 (5) Å
c = 18.432 (8) Å
V = 2447.9 (19) Å^3
Z = 8
$F(000)$ = 1136
D_x = 1.472 Mg m^{-3}
Mo $K\alpha$ radiation, λ = 0.71075 Å
Cell parameters from 3248 reflections
θ = 3.3–27.5°
μ = 0.11 mm^{-1}
T = 143 K
Block-like, colorless
0.31 × 0.20 × 0.14 mm

Data collection

Rigaku Pilatus 200K diffractometer
Radiation source: Rotating Anode
profile data from ω–scans
Absorption correction: numerical (Busing et al., 1957; Coppens *et al.*, 1965)
T_{min} = 0.985, T_{max} = 0.991
37607 measured reflections
5347 independent reflections
4234 reflections with $I > 2\sigma(I)$
R_{int} = 0.044
θ_{max} = 27.5°, θ_{min} = 3.3°
h = −14→14
k = −15→11
l = −23→23

Refinement

Refinement on F^2
Least-squares matrix: full
$R[F^2 > 2\sigma(F^2)]$ = 0.034
$wR(F^2)$ = 0.077
S = 0.92
5347 reflections
362 parameters
1 restraint
Primary atom site location: dual
Secondary atom site location: difference Fourier map
Hydrogen site location: inferred from neighbouring sites
H-atom parameters constrained
$w = 1/[\sigma^2(F_o^2) + (0.0499P)^2]$ where $P = (F_o^2 + 2F_c^2)/3$
$(\Delta/\sigma)_{max} < 0.001$
$\Delta\rho_{max}$ = 0.25 e Å^{-3}
$\Delta\rho_{min}$ = −0.17 e Å^{-3}
Absolute structure: Refined as an inversion twin

Special details

Geometry. All esds (except the esd in the dihedral angle between two l.s. planes) are estimated using the full covariance matrix. The cell esds are taken into account individually in the estimation of esds in distances, angles and torsion angles; correlations between esds in cell parameters are only used when they are defined by crystal symmetry. An approximate (isotropic) treatment of cell esds is used for estimating esds involving l.s. planes.

Refinement. Refined as a 2-component inversion twin.

Fractional atomic coordinates and isotropic or equivalent isotropic displacement parameters (Å²)

	x	*y*	*z*	U_{iso}*/U_{eq}
O1	−0.11945 (18)	0.50167 (16)	0.64782 (12)	0.0307 (5)
O2	−0.06787 (16)	0.49189 (14)	0.51523 (11)	0.0192 (4)
O1A	0.13975 (17)	1.02313 (17)	0.34982 (11)	0.0303 (5)
O3	0.22361 (16)	0.36364 (15)	0.43955 (10)	0.0289 (4)
O2A	0.18982 (15)	1.02605 (14)	0.48285 (9)	0.0199 (4)
O4	0.07162 (16)	0.70987 (14)	0.40423 (9)	0.0260 (4)
O3A	0.48025 (15)	1.12960 (14)	0.56683 (10)	0.0262 (4)
O4A	0.32226 (16)	0.78153 (15)	0.58545 (10)	0.0278 (4)
N1	0.16171 (19)	0.53901 (17)	0.40756 (12)	0.0206 (5)
N1A	0.40913 (17)	0.95429 (17)	0.59153 (11)	0.0194 (4)
C1	0.0028 (3)	0.4713 (3)	0.63137 (15)	0.0309 (7)
H1	0.060539	0.450985	0.670915	0.037*
C2	−0.0374 (2)	0.5851 (2)	0.62233 (13)	0.0248 (6)
H2	−0.008089	0.645671	0.655227	0.030*
C1A	0.2652 (2)	1.0441 (2)	0.36676 (14)	0.0281 (6)
H1A	0.325082	1.061602	0.327794	0.034*
C3	0.0226 (2)	0.4313 (2)	0.55475 (14)	0.0232 (6)
H3	0.021379	0.348487	0.548042	0.028*
C2A	0.2146 (2)	0.9333 (2)	0.37433 (13)	0.0236 (6)
H2A	0.238647	0.871535	0.340889	0.028*
C4	−0.0389 (2)	0.6008 (2)	0.54095 (13)	0.0186 (5)
H4	−0.092383	0.661999	0.522908	0.022*
C3A	0.2857 (2)	1.0810 (2)	0.44490 (14)	0.0221 (5)
H3A	0.291239	1.163377	0.452598	0.027*
C5	0.1396 (3)	0.4906 (2)	0.52978 (15)	0.0212 (7)
H5	0.205042	0.486004	0.567012	0.025*
C4A	0.2109 (2)	0.9161 (2)	0.45570 (14)	0.0190 (5)
H4A	0.152631	0.858144	0.472839	0.023*
C6	0.0943 (2)	0.61035 (19)	0.51891 (13)	0.0187 (5)
H6	0.139769	0.666128	0.548568	0.022*
C5A	0.3964 (2)	1.0131 (2)	0.47013 (15)	0.0172 (6)
H5A	0.464537	1.016201	0.434641	0.021*
C7	0.1816 (2)	0.4530 (2)	0.45617 (15)	0.0209 (5)
C6A	0.3429 (2)	0.89612 (19)	0.47726 (12)	0.0173 (5)
H6A	0.383732	0.841027	0.444741	0.021*
C8	0.1057 (2)	0.6304 (2)	0.43823 (13)	0.0195 (5)
C7A	0.4354 (2)	1.0435 (2)	0.54662 (14)	0.0203 (5)
C9	0.1925 (2)	0.5348 (2)	0.33081 (13)	0.0278 (6)

H9A	0.118912	0.548682	0.301724	0.033*
H9B	0.222156	0.459083	0.318786	0.033*
C8A	0.3552 (2)	0.8660 (2)	0.55583 (13)	0.0190 (5)
C10	0.2880 (2)	0.6195 (2)	0.31034 (13)	0.0209 (6)
C9A	0.4347 (2)	0.9512 (2)	0.66915 (13)	0.0251 (6)
H9AA	0.360486	0.929416	0.695550	0.030*
H9AB	0.457937	1.026788	0.685621	0.030*
C11	0.2762 (2)	0.6842 (2)	0.24819 (13)	0.0230 (6)
H11	0.208689	0.674147	0.217123	0.028*
C10A	0.5341 (2)	0.8706 (2)	0.68755 (13)	0.0217 (6)
C12	0.3623 (2)	0.7627 (2)	0.23165 (12)	0.0240 (6)
H12	0.353218	0.807033	0.189268	0.029*
C11A	0.6367 (2)	0.8630 (2)	0.64473 (15)	0.0325 (7)
H11A	0.643953	0.908179	0.602619	0.039*
C13	0.4613 (2)	0.7782 (2)	0.27534 (14)	0.0250 (6)
H13	0.519662	0.833509	0.263768	0.030*
C12A	0.7284 (3)	0.7901 (2)	0.66289 (16)	0.0373 (7)
H12A	0.798131	0.785277	0.633028	0.045*
C14	0.4751 (2)	0.7121 (2)	0.33665 (13)	0.0257 (6)
H14	0.544037	0.721240	0.366729	0.031*
C13A	0.7196 (2)	0.7244 (2)	0.72402 (15)	0.0296 (7)
H13A	0.782799	0.674282	0.736315	0.036*
C15	0.3898 (2)	0.6336 (2)	0.35402 (13)	0.0248 (6)
H15	0.399988	0.588673	0.396010	0.030*
C14A	0.6184 (2)	0.7320 (2)	0.76712 (12)	0.0255 (6)
H14A	0.612238	0.687524	0.809637	0.031*
C15A	0.5263 (2)	0.8034 (2)	0.74899 (13)	0.0219 (6)
H15A	0.456375	0.807033	0.778732	0.026*

Atomic displacement parameters (Å²)

	U^{11}	U^{22}	U^{33}	U^{12}	U^{13}	U^{23}
O1	0.0230 (10)	0.0431 (13)	0.0261 (11)	−0.0020 (8)	0.0078 (9)	0.0068 (8)
O2	0.0153 (9)	0.0201 (10)	0.0223 (10)	−0.0016 (7)	−0.0032 (8)	−0.0013 (7)
O1A	0.0248 (11)	0.0368 (11)	0.0294 (12)	0.0011 (9)	−0.0088 (10)	0.0067 (9)
O3	0.0239 (10)	0.0221 (10)	0.0408 (11)	0.0029 (8)	−0.0028 (8)	−0.0060 (8)
O2A	0.0144 (9)	0.0215 (10)	0.0238 (10)	0.0039 (7)	0.0005 (8)	−0.0034 (7)
O4	0.0361 (10)	0.0176 (10)	0.0243 (9)	−0.0017 (8)	−0.0021 (8)	0.0039 (7)
O3A	0.0225 (9)	0.0225 (10)	0.0335 (10)	−0.0046 (8)	0.0003 (7)	−0.0047 (8)
O4A	0.0331 (10)	0.0214 (10)	0.0291 (10)	−0.0024 (8)	−0.0034 (8)	0.0064 (8)
N1	0.0227 (11)	0.0190 (12)	0.0201 (11)	−0.0023 (10)	0.0026 (9)	−0.0018 (9)
N1A	0.0196 (11)	0.0203 (12)	0.0183 (11)	0.0020 (10)	−0.0011 (9)	−0.0005 (9)
C1	0.0184 (13)	0.051 (2)	0.0235 (16)	0.0057 (13)	0.0007 (12)	0.0142 (13)
C2	0.0180 (13)	0.0338 (16)	0.0227 (13)	−0.0095 (12)	0.0010 (10)	−0.0020 (11)
C1A	0.0213 (14)	0.0369 (17)	0.0261 (16)	−0.0007 (13)	−0.0019 (11)	0.0088 (12)
C3	0.0209 (13)	0.0184 (13)	0.0304 (15)	0.0000 (11)	0.0035 (11)	0.0079 (11)
C2A	0.0222 (14)	0.0314 (16)	0.0173 (13)	0.0045 (11)	−0.0014 (10)	−0.0011 (11)
C4	0.0184 (12)	0.0165 (13)	0.0208 (12)	−0.0012 (10)	−0.0024 (10)	−0.0048 (9)

C3A	0.0210 (13)	0.0179 (13)	0.0275 (14)	−0.0051 (11)	−0.0004 (11)	0.0060 (11)
C5	0.0175 (15)	0.0249 (15)	0.0211 (16)	0.0007 (10)	−0.0036 (12)	0.0030 (10)
C4A	0.0183 (12)	0.0176 (13)	0.0211 (12)	−0.0018 (10)	−0.0018 (10)	−0.0012 (10)
C6	0.0177 (12)	0.0182 (14)	0.0202 (12)	−0.0039 (10)	−0.0026 (10)	0.0002 (10)
C5A	0.0129 (13)	0.0209 (14)	0.0179 (15)	0.0008 (10)	0.0007 (12)	0.0019 (10)
C7	0.0113 (11)	0.0197 (15)	0.0318 (14)	−0.0027 (11)	−0.0014 (11)	0.0016 (11)
C6A	0.0159 (12)	0.0169 (13)	0.0192 (12)	0.0016 (10)	0.0004 (10)	−0.0041 (10)
C8	0.0187 (13)	0.0182 (13)	0.0217 (12)	−0.0066 (11)	−0.0018 (10)	−0.0016 (10)
C7A	0.0118 (11)	0.0228 (15)	0.0264 (13)	0.0026 (11)	0.0003 (10)	−0.0047 (11)
C9	0.0336 (15)	0.0322 (17)	0.0176 (13)	−0.0053 (13)	0.0027 (11)	−0.0065 (12)
C8A	0.0163 (12)	0.0179 (14)	0.0230 (13)	0.0051 (10)	−0.0005 (10)	−0.0002 (10)
C10	0.0215 (13)	0.0220 (14)	0.0192 (13)	0.0003 (10)	0.0041 (10)	−0.0056 (10)
C9A	0.0297 (15)	0.0281 (16)	0.0176 (13)	0.0058 (13)	−0.0043 (11)	−0.0019 (11)
C11	0.0217 (13)	0.0290 (15)	0.0182 (13)	0.0043 (12)	0.0000 (11)	−0.0049 (11)
C10A	0.0220 (14)	0.0248 (14)	0.0182 (13)	−0.0013 (11)	−0.0037 (10)	−0.0030 (10)
C12	0.0267 (14)	0.0280 (16)	0.0173 (15)	0.0046 (12)	0.0053 (12)	0.0015 (11)
C11A	0.0259 (14)	0.0421 (18)	0.0295 (14)	0.0033 (13)	0.0058 (12)	0.0143 (13)
C13	0.0207 (14)	0.0252 (15)	0.0290 (15)	0.0010 (12)	0.0054 (11)	0.0001 (11)
C12A	0.0253 (15)	0.0483 (19)	0.0383 (17)	0.0042 (14)	0.0106 (12)	0.0181 (15)
C14	0.0208 (12)	0.0330 (15)	0.0232 (13)	0.0009 (12)	−0.0006 (10)	−0.0003 (11)
C13A	0.0201 (14)	0.0348 (17)	0.0340 (16)	0.0031 (12)	−0.0027 (12)	0.0079 (13)
C15	0.0270 (13)	0.0281 (15)	0.0195 (12)	0.0031 (12)	−0.0006 (10)	0.0037 (11)
C14A	0.0291 (15)	0.0255 (16)	0.0220 (15)	−0.0054 (12)	−0.0001 (12)	0.0046 (11)
C15A	0.0188 (12)	0.0295 (15)	0.0173 (13)	−0.0035 (12)	0.0008 (10)	−0.0039 (11)

Geometric parameters (Å, º)

O1—C2	1.431 (3)	C4A—C6A	1.534 (3)
O1—C1	1.435 (3)	C4A—H4A	1.0000
O2—C4	1.426 (3)	C6—C8	1.512 (3)
O2—C3	1.436 (3)	C6—H6	1.0000
O1A—C2A	1.432 (3)	C5A—C7A	1.519 (4)
O1A—C1A	1.446 (3)	C5A—C6A	1.528 (4)
O3—C7	1.207 (3)	C5A—H5A	1.0000
O2A—C4A	1.429 (3)	C6A—C8A	1.499 (3)
O2A—C3A	1.432 (3)	C6A—H6A	1.0000
O4—C8	1.201 (3)	C9—C10	1.514 (3)
O3A—C7A	1.204 (3)	C9—H9A	0.9900
O4A—C8A	1.207 (3)	C9—H9B	0.9900
N1—C8	1.380 (3)	C10—C11	1.389 (3)
N1—C7	1.384 (3)	C10—C15	1.396 (3)
N1—C9	1.456 (3)	C9A—C10A	1.505 (3)
N1A—C8A	1.382 (3)	C9A—H9AA	0.9900
N1A—C7A	1.383 (3)	C9A—H9AB	0.9900
N1A—C9A	1.459 (3)	C11—C12	1.374 (4)
C1—C2	1.445 (4)	C11—H11	0.9500
C1—C3	1.508 (4)	C10A—C11A	1.387 (4)
C1—H1	1.0000	C10A—C15A	1.392 (3)

C2—C4	1.512 (3)	C12—C13	1.373 (4)
C2—H2	1.0000	C12—H12	0.9500
C1A—C2A	1.448 (4)	C11A—C12A	1.381 (4)
C1A—C3A	1.524 (4)	C11A—H11A	0.9500
C1A—H1A	1.0000	C13—C14	1.389 (4)
C3—C5	1.548 (4)	C13—H13	0.9500
C3—H3	1.0000	C12A—C13A	1.378 (4)
C2A—C4A	1.514 (4)	C12A—H12A	0.9500
C2A—H2A	1.0000	C14—C15	1.371 (4)
C4—C6	1.534 (3)	C14—H14	0.9500
C4—H4	1.0000	C13A—C14A	1.377 (4)
C3A—C5A	1.543 (3)	C13A—H13A	0.9500
C3A—H3A	1.0000	C15—H15	0.9500
C5—C7	1.504 (4)	C14A—C15A	1.373 (4)
C5—C6	1.534 (3)	C14A—H14A	0.9500
C5—H5	1.0000	C15A—H15A	0.9500

C2—O1—C1	60.56 (19)	C7A—C5A—C3A	112.3 (2)
C4—O2—C3	97.91 (19)	C6A—C5A—C3A	101.7 (2)
C2A—O1A—C1A	60.39 (17)	C7A—C5A—H5A	112.5
C4A—O2A—C3A	97.55 (18)	C6A—C5A—H5A	112.5
C8—N1—C7	113.4 (2)	C3A—C5A—H5A	112.5
C8—N1—C9	122.1 (2)	O3—C7—N1	123.9 (3)
C7—N1—C9	124.5 (2)	O3—C7—C5	127.9 (2)
C8A—N1A—C7A	113.5 (2)	N1—C7—C5	108.2 (2)
C8A—N1A—C9A	122.1 (2)	C8A—C6A—C5A	105.6 (2)
C7A—N1A—C9A	124.5 (2)	C8A—C6A—C4A	112.0 (2)
O1—C1—C2	59.59 (17)	C5A—C6A—C4A	101.75 (19)
O1—C1—C3	114.6 (2)	C8A—C6A—H6A	112.3
C2—C1—C3	103.7 (2)	C5A—C6A—H6A	112.3
O1—C1—H1	120.8	C4A—C6A—H6A	112.3
C2—C1—H1	120.8	O4—C8—N1	123.8 (2)
C3—C1—H1	120.8	O4—C8—C6	127.8 (2)
O1—C2—C1	59.84 (17)	N1—C8—C6	108.3 (2)
O1—C2—C4	114.0 (2)	O3A—C7A—N1A	124.3 (2)
C1—C2—C4	103.6 (2)	O3A—C7A—C5A	127.6 (2)
O1—C2—H2	121.0	N1A—C7A—C5A	108.1 (2)
C1—C2—H2	121.0	N1—C9—C10	112.5 (2)
C4—C2—H2	121.0	N1—C9—H9A	109.1
O1A—C1A—C2A	59.31 (17)	C10—C9—H9A	109.1
O1A—C1A—C3A	113.4 (2)	N1—C9—H9B	109.1
C2A—C1A—C3A	103.5 (2)	C10—C9—H9B	109.1
O1A—C1A—H1A	121.3	H9A—C9—H9B	107.8
C2A—C1A—H1A	121.3	O4A—C8A—N1A	123.9 (2)
C3A—C1A—H1A	121.3	O4A—C8A—C6A	127.7 (2)
O2—C3—C1	102.3 (2)	N1A—C8A—C6A	108.4 (2)
O2—C3—C5	101.59 (19)	C11—C10—C15	118.9 (2)
C1—C3—C5	104.7 (2)	C11—C10—C9	121.0 (2)

O2—C3—H3	115.5	C15—C10—C9	120.1 (2)
C1—C3—H3	115.5	N1A—C9A—C10A	112.3 (2)
C5—C3—H3	115.5	N1A—C9A—H9AA	109.1
O1A—C2A—C1A	60.30 (17)	C10A—C9A—H9AA	109.1
O1A—C2A—C4A	113.5 (2)	N1A—C9A—H9AB	109.1
C1A—C2A—C4A	103.3 (2)	C10A—C9A—H9AB	109.1
O1A—C2A—H2A	121.1	H9AA—C9A—H9AB	107.9
C1A—C2A—H2A	121.1	C12—C11—C10	120.0 (2)
C4A—C2A—H2A	121.1	C12—C11—H11	120.0
O2—C4—C2	102.6 (2)	C10—C11—H11	120.0
O2—C4—C6	101.35 (18)	C11A—C10A—C15A	118.4 (2)
C2—C4—C6	105.2 (2)	C11A—C10A—C9A	120.9 (2)
O2—C4—H4	115.3	C15A—C10A—C9A	120.6 (2)
C2—C4—H4	115.3	C13—C12—C11	121.1 (2)
C6—C4—H4	115.3	C13—C12—H12	119.4
O2A—C3A—C1A	102.6 (2)	C11—C12—H12	119.4
O2A—C3A—C5A	101.52 (19)	C12A—C11A—C10A	120.4 (2)
C1A—C3A—C5A	104.5 (2)	C12A—C11A—H11A	119.8
O2A—C3A—H3A	115.5	C10A—C11A—H11A	119.8
C1A—C3A—H3A	115.5	C12—C13—C14	119.2 (2)
C5A—C3A—H3A	115.5	C12—C13—H13	120.4
C7—C5—C6	105.3 (2)	C14—C13—H13	120.4
C7—C5—C3	113.0 (2)	C13A—C12A—C11A	120.5 (3)
C6—C5—C3	101.2 (2)	C13A—C12A—H12A	119.8
C7—C5—H5	112.2	C11A—C12A—H12A	119.8
C6—C5—H5	112.2	C15—C14—C13	120.4 (2)
C3—C5—H5	112.2	C15—C14—H14	119.8
O2A—C4A—C2A	103.0 (2)	C13—C14—H14	119.8
O2A—C4A—C6A	102.10 (18)	C14A—C13A—C12A	119.5 (2)
C2A—C4A—C6A	104.6 (2)	C14A—C13A—H13A	120.3
O2A—C4A—H4A	115.1	C12A—C13A—H13A	120.3
C2A—C4A—H4A	115.1	C14—C15—C10	120.4 (2)
C6A—C4A—H4A	115.1	C14—C15—H15	119.8
C8—C6—C4	110.64 (19)	C10—C15—H15	119.8
C8—C6—C5	104.5 (2)	C15A—C14A—C13A	120.4 (2)
C4—C6—C5	102.1 (2)	C15A—C14A—H14A	119.8
C8—C6—H6	112.9	C13A—C14A—H14A	119.8
C4—C6—H6	112.9	C14A—C15A—C10A	120.8 (2)
C5—C6—H6	112.9	C14A—C15A—H15A	119.6
C7A—C5A—C6A	104.5 (2)	C10A—C15A—H15A	119.6

C2—O1—C1—C3	−92.0 (3)	C3—C5—C7—N1	108.6 (2)
C1—O1—C2—C4	92.3 (2)	C7A—C5A—C6A—C8A	−0.5 (3)
C3—C1—C2—O1	110.7 (2)	C3A—C5A—C6A—C8A	−117.5 (2)
O1—C1—C2—C4	−110.0 (2)	C7A—C5A—C6A—C4A	116.5 (2)
C3—C1—C2—C4	0.6 (3)	C3A—C5A—C6A—C4A	−0.5 (2)
C2A—O1A—C1A—C3A	−92.2 (2)	O2A—C4A—C6A—C8A	78.5 (2)
C4—O2—C3—C1	51.7 (2)	C2A—C4A—C6A—C8A	−174.3 (2)

C4—O2—C3—C5	−56.3 (2)
O1—C1—C3—O2	30.2 (3)
C2—C1—C3—O2	−32.3 (3)
O1—C1—C3—C5	135.8 (2)
C2—C1—C3—C5	73.3 (2)
C1A—O1A—C2A—C4A	92.4 (2)
C3A—C1A—C2A—O1A	109.5 (2)
O1A—C1A—C2A—C4A	−109.7 (2)
C3A—C1A—C2A—C4A	−0.2 (3)
C3—O2—C4—C2	−51.4 (2)
C3—O2—C4—C6	57.2 (2)
O1—C2—C4—O2	−31.2 (3)
C1—C2—C4—O2	31.6 (2)
O1—C2—C4—C6	−136.8 (2)
C1—C2—C4—C6	−74.1 (2)
C4A—O2A—C3A—C1A	51.5 (2)
C4A—O2A—C3A—C5A	−56.4 (2)
O1A—C1A—C3A—O2A	30.2 (3)
C2A—C1A—C3A—O2A	−31.8 (3)
O1A—C1A—C3A—C5A	135.8 (2)
C2A—C1A—C3A—C5A	73.8 (3)
O2—C3—C5—C7	−79.3 (2)
C1—C3—C5—C7	174.6 (2)
O2—C3—C5—C6	32.9 (2)
C1—C3—C5—C6	−73.3 (2)
C3A—O2A—C4A—C2A	−51.9 (2)
C3A—O2A—C4A—C6A	56.4 (2)
O1A—C2A—C4A—O2A	−30.8 (3)
C1A—C2A—C4A—O2A	32.4 (3)
O1A—C2A—C4A—C6A	−137.2 (2)
C1A—C2A—C4A—C6A	−74.0 (2)
O2—C4—C6—C8	75.3 (2)
C2—C4—C6—C8	−178.1 (2)
O2—C4—C6—C5	−35.4 (2)
C2—C4—C6—C5	71.2 (2)
C7—C5—C6—C8	3.8 (3)
C3—C5—C6—C8	−114.0 (2)
C7—C5—C6—C4	119.1 (2)
C3—C5—C6—C4	1.3 (2)
O2A—C3A—C5A—C7A	−76.8 (2)
C1A—C3A—C5A—C7A	176.8 (2)
O2A—C3A—C5A—C6A	34.4 (2)
C1A—C3A—C5A—C6A	−72.0 (2)
C8—N1—C7—O3	175.9 (2)
C9—N1—C7—O3	−2.3 (4)
C8—N1—C7—C5	−2.7 (3)
C9—N1—C7—C5	179.0 (2)
C6—C5—C7—O3	−179.6 (2)
O2A—C4A—C6A—C5A	−33.8 (2)
C2A—C4A—C6A—C5A	73.3 (2)
C7—N1—C8—O4	−173.7 (2)
C9—N1—C8—O4	4.5 (4)
C7—N1—C8—C6	5.3 (3)
C9—N1—C8—C6	−176.4 (2)
C4—C6—C8—O4	64.3 (3)
C5—C6—C8—O4	173.5 (2)
C4—C6—C8—N1	−114.7 (2)
C5—C6—C8—N1	−5.5 (3)
C8A—N1A—C7A—O3A	178.5 (2)
C9A—N1A—C7A—O3A	−1.5 (4)
C8A—N1A—C7A—C5A	−0.8 (3)
C9A—N1A—C7A—C5A	179.3 (2)
C6A—C5A—C7A—O3A	−178.4 (2)
C3A—C5A—C7A—O3A	−69.0 (3)
C6A—C5A—C7A—N1A	0.8 (3)
C3A—C5A—C7A—N1A	110.2 (2)
C8—N1—C9—C10	66.0 (3)
C7—N1—C9—C10	−116.0 (3)
C7A—N1A—C8A—O4A	−178.0 (2)
C9A—N1A—C8A—O4A	1.9 (3)
C7A—N1A—C8A—C6A	0.4 (3)
C9A—N1A—C8A—C6A	−179.6 (2)
C5A—C6A—C8A—O4A	178.5 (2)
C4A—C6A—C8A—O4A	68.5 (3)
C5A—C6A—C8A—N1A	0.1 (2)
C4A—C6A—C8A—N1A	−109.8 (2)
N1—C9—C10—C11	−135.3 (2)
N1—C9—C10—C15	44.8 (3)
C8A—N1A—C9A—C10A	69.9 (3)
C7A—N1A—C9A—C10A	−110.1 (3)
C15—C10—C11—C12	−1.8 (4)
C9—C10—C11—C12	178.2 (2)
N1A—C9A—C10A—C11A	41.6 (3)
N1A—C9A—C10A—C15A	−139.7 (2)
C10—C11—C12—C13	0.5 (4)
C15A—C10A—C11A—C12A	0.1 (4)
C9A—C10A—C11A—C12A	178.8 (3)
C11—C12—C13—C14	0.9 (4)
C10A—C11A—C12A—C13A	−0.3 (5)
C12—C13—C14—C15	−1.2 (4)
C11A—C12A—C13A—C14A	−0.1 (4)
C13—C14—C15—C10	−0.1 (4)
C11—C10—C15—C14	1.6 (4)
C9—C10—C15—C14	−178.5 (2)
C12A—C13A—C14A—C15A	0.8 (4)
C13A—C14A—C15A—C10A	−1.0 (4)

C3—C5—C7—O3	−70.0 (3)	C11A—C10A—C15A—C14A	0.5 (4)
C6—C5—C7—N1	−0.9 (3)	C9A—C10A—C15A—C14A	−178.2 (2)